Structures of Side Chain Liquid Crystalline Poly(silylenemethylene)s

Soo-Young Park,[†,§] Tao Zhang,[‡] L. V. Interrante,[‡] and B. L. Farmer*[,†]

Air Force Research Laboratory, Materials and Manufacturing Directorate, Wright-Patterson Air Force Base, Ohio 45433-7750, and Department of Chemistry, Rensselaer Polytechnic Institute, Troy, New York 12180-3590

Received March 13, 2001

ABSTRACT: The structures of side chain liquid crystalline poly(silylenemethylene)s (−($SiCH_3R−CH_2$)−: R = $O(CH_2)_NO−Ph−Ph$, Ph = phenyl) (PSM-*N*; *N* = 3, 6, 8, 11) have been studied by X-ray diffraction, differential scanning calorimetry (DSC), polarized optical microscopy, and transmission electron microscopy (TEM). DSC study showed that PSM-*N*s have multiple transitions that are dependent on the side chain length. All PSM-*N*s studied show a series of sharp equatorial reflections in the X-ray fiber pattern at room temperature, a characteristic of well-ordered smectic phases. Layered smectic structures of PSM-*N*s persist up to the isotropic temperature during heating, although the specific kinds of smectic phases changed. In each, the layer thickness corresponds to the single side chain length and increases with slope of ∼1.3 Å per methylene spacer. This is a single-layer structure. For PSM-3 and PSM-6, the mesogens pack in a two-dimensional orthorhombic cell, a characteristic of a smectic E (S_E) phase, with dimensions *a* = 8.14 Å and *b* = 5.14 Å. The S_E phase of PSM-3 and PSM-6 converts directly to the isotropic phase. For PSM-8 and PSM-11, the mesogens pack in a hexagonal smectic B (S_B) cell at room temperature. This is manifest from the hexagonal six-point arrangement of reflections at *d* = 4.4 Å in the X-ray fiber pattern. During room temperature annealing, PSM-8 and PSM-11 crystallize into orthorhombic cells with parameters *a* = 8.80 Å, *b* = 5.08 Å, *c* = 50.8 Å for PSM-8 and *a* = 8.90 Å, *b* = 5.14 Å, *c* = 58.6 Å for PSM-11. Upon heating, the crystalline structures change to smectic A (S_A) before becoming isotropic. Micrographs of PSM-11 show a layered structure with thickness matching that observed in X-ray pattern.

1. Introduction

Side chain liquid crystal polymers have great potential as new materials for electronic displays and nonlinear optics.[1] The occurrence of a liquid crystal phase depends on the ability of the mesogenic groups to arrange themselves anisotropically. Their ordering is affected both by the flexible spacer connecting them to the polymer backbone and by the flexibility of the backbone itself. In this respect, polysiloxanes are good candidates for the backbone of side chain liquid crystal polymers because of the low rotational energy barrier of the Si−O bond.[2] However, they also tend to have lower glass transition temperatures than their carbon backbone (acrylate/methacrylate) counterparts.[3]

Poly(silylenemethylene)s, $[SiRR'CH_2]_n$, (PSMs), having a backbone of alternating Si and C atoms have been synthesized and characterized.[4−7] Si−C bonds have a relatively flat torsional energy surface, but their glass transition temperatures are typically ∼40 °C higher than their polysiloxane counterparts. The Si−C backbone is also known to provide thermal stability similar to, or even better than, that of the polysiloxanes.[8] Moreover, the Si−C backbone offers the prospect of improved backbone hydrolytic stability over the polysiloxanes. Thus, PSMs might be superior candidates for side chain liquid crystal polymers. Recently, PSM-based side chain liquid crystal polymers (−($SiCH_3R−CH_2$)−: R = $O(CH_2)_NO−Ph−Ph$, Ph = phenyl, *N* = 3, 6, 8, 11) (PSM-*N*) have been prepared.[9] Highly ordered smectic phases from PSM-*N*s were observed. The highly ordered phases, such as smectic B (S_B), smectic E (S_E), smectic F (S_F), smectic G (S_G), smectic I (S_I), and smectic J (S_J), are characterized by the particular arrangement of the mesogenic groups within the layers: S_B with hexagonal packing of the mesogens, S_E with an orthorhombic cell with the mesogens normal to the layers, S_F, S_G, S_I, and S_J with a tilted arrangement of the mesogenic groups.[10−13] In this paper, we report the structure of PSM-*N*s, studied by X-ray, differential scanning calorimetry (DSC), polarized optical microscopy, and transmission electron microscopy (TEM).

2. Experiment

The synthesis and general characterization of the specimens of PSM-*N*s were reported in ref 9. Fiber specimens for X-ray work were prepared by drawing (with tweezers) the isotropic melt on a slide glass at 120 °C. Wide-angle X-ray diffraction patterns were recorded on both Kodak direct exposure film and a phosphor image plate (Molecular Dynamics) in a Statton camera. Monochromatic Cu Kα radiation from a rotating anode X-ray generator operating at 40 kV and 240 mA was used. The sample to film distance was calibrated by SiO_2 powders. X-ray patterns at high temperatures were obtained using a heating accessory for the Statton camera. DSC experiments were carried out in a Perkin-Elmer DSC-7. The temperature and heat flow scales were calibrated using standard materials. The sample size was ∼1.5 mg. For cooling scans, the samples were heated above their isotropic temperatures for 2 min and then cooled to 20 °C at a rate of −10 °C/min. For heating scans, the samples were first cooled from 120 °C (isotropic state) to 20 °C at a rate of −10 °C/min and then heated at a rate of 10 °C/min. The transition temperatures were determined from the maxima in the transition curves. Liquid crystalline textures were observed using an optical microscope (Leitz, Ortholux) with crossed polarizing filters and a Mettler hot stage (FP-80). The samples were melted into the isotropic state (∼120 °C) between slide glasses, cooled to the selected temperatures, and annealed for a day. Samples suitable for TEM were prepared by casting thin films on carbon-coated glass cover slides. A drop of 0.05 wt % solution of polymer in toluene was evaporated to dryness, melted, crystallized at the desired

[†] Wright-Patterson Air Force Base.
[‡] Rensselaer Polytechnic Institute.
* To whom correspondence should be addressed.
[§] Present address: Kyungpook National University.

10.1021/ma010449s CCC: $22.00
Published on Web 02/28/2002

Table 1. Transition Temperatures and Enthalpies of PSM-*N*s during Heating and Cooling

		PSM-3		PSM-6		PSM-8		PSM-11	
		temp (°C)	ΔH (J/g)	temp (°C)	ΔH (J/g)	temp (°C)	ΔH (J/g)	temp (°C)	ΔH (J/g)
cooling	T_{c1}	66.6	16.9	88.5	20.6	89.5	15.7	84.5	16.0
	T_{c2}					61.5	1.6	48.8	1.4
	T_{c3}							27.3	11.0
heating	T_{h1}	83.0	14.1	95.5	13.4	95.3	15.8	91.8	15.0
	T_{h2}			92.5	7.9	64.5	1.3	64.8	12
	T_{h3}							32.3	
	T_{ex1}							41.8	

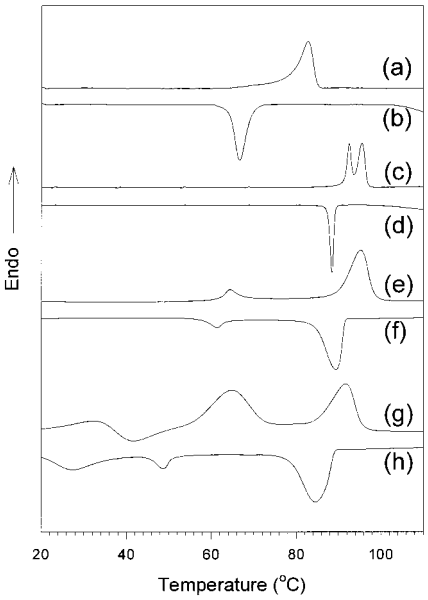

Figure 1. DSC thermograms for (a) PSM-3 during heating, (b) PSM-3 during cooling, (c) PSM-6 during heating, (d) PSM-6 during cooling, (e) PSM-8 during heating, (f) PSM-8 during cooling, (g) PSM-11 during heating, and (h) PSM-11 during cooling. Heating/cooling rate was ±10 °C.

temperature in a Mettler hot stage, and then stained with RuO_4 (0.2%) for 20 s.

3. Results and Discussion

Thermal Analysis. Figure 1 shows DSC heating and cooling thermograms for PSM-3, PSM-6, PSM-8, and PSM-11. The transition temperatures and enthalpies are summarized in Table 1. It can be seen that the spacer length affects not only the transition temperatures but also the number of transitions observed.

The number of transitions during heating generally increases with increasing spacer length. The highest transition temperatures (T_{h1}) and enthalpies (ΔH_{h1}) during heating are similar although T_{h1} of PSM-3 (83 °C) is a little lower than the others (∼94 °C). That this transition is related to the isotropic transition was confirmed through polarized optical microscopy. The large enthalpy at T_{h1} indicates that the phase preceding the isotropic phase may be highly ordered and probably smectic. (The typical enthalpy of a nematic to isotropic transition is of the order of ∼2 J/g.[3]) For PSM-8, the enthalpies at T_{h2} and T_{c2} (∼1.5 J/g) (see table for designations) are much less than those at T_{h1} and T_{c1} (∼16 J/g), suggesting that the structural change at the T_{h2} transition is relatively minor. PSM-11 shows three transitions during both heating and cooling and one exothermic peak during heating. The transition at T_{h2}, following the exothermic transition (T_{ex1}), has much larger enthalpy (∼12 J/g) than that at T_{c2} (∼1.4 J/g).

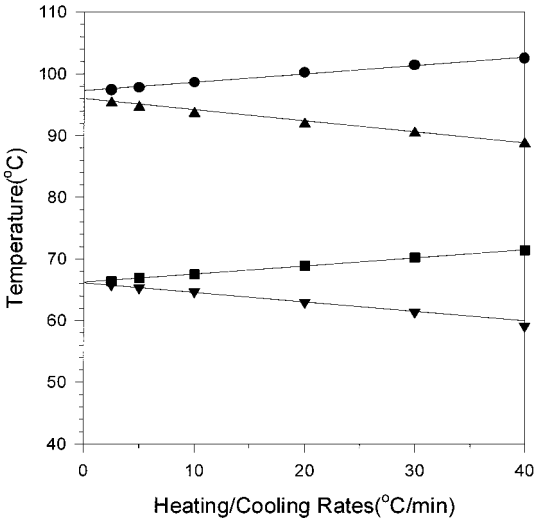

Figure 2. T_{h1} (●), T_{h2} (■), T_{c1} (▲), and T_{c2} (▼) at various heating/cooling rates for PSM-8.

The increased enthalpy suggests that the structure produced by the exothermic reaction at T_{ex1} takes part in the structural changes at T_{h2}.

Figure 2 shows T_{h1}, T_{h2}, T_{c1}, and T_{c2} at different heating/cooling rates for PSM-8. (Similar plots for PSM-3, PSM-6, and PSM-11 are omitted here, and their results are explained in the text.) The transition temperatures are dependent on the heating/cooling rates, increasing as the heating rate increases and decreasing as the cooling rate increases. The difference between heating and cooling transition temperatures decreases as the heating/cooling rates decrease. Equilibrium transition temperatures ($T°$) can be obtained by extrapolating to zero heating/cooling rate. In the case of PSM-3, $T_{h1}°$ is 83 °C and $T_{c1}°$ is 72 °C, giving a degree of supercooling (at zero heating/cooling rate), $\Delta T_1°$, of 11 °C. $\Delta T_1°$s are 4, 1, and 1 °C for PSM-6, PSM-8, and PSM-11, respectively. $\Delta T_1°$ decreases as spacer length increases. One characteristic of liquid crystalline materials is that the degree of supercooling of a liquid crystal phase is smaller than that of a crystalline material and that of a high-order liquid crystal phase is larger than that of a low-order liquid crystal phase. For PSM-8 and PSM-11, $\Delta T_1°$s are small, suggesting that the transition at T_1 is related to relatively low order liquid crystal structures. The $\Delta T_1°$s for PSM-3 and PSM-6 are 11 and 4 °C, suggesting a crystal or high-order smectic phase is involved in their transitions. For the second transition, $\Delta T_2°$ for PSM-8 is 0 °C, whereas that for PSM-11 is 11 °C. This large $\Delta T_2°$ for PSM-11 is a result of crystallization at the exothermic reaction. X-ray, optical microscopy, and TEM methods were employed to study the specific structures of the PSM-*N*s and the nature of the structural changes during the transitions.

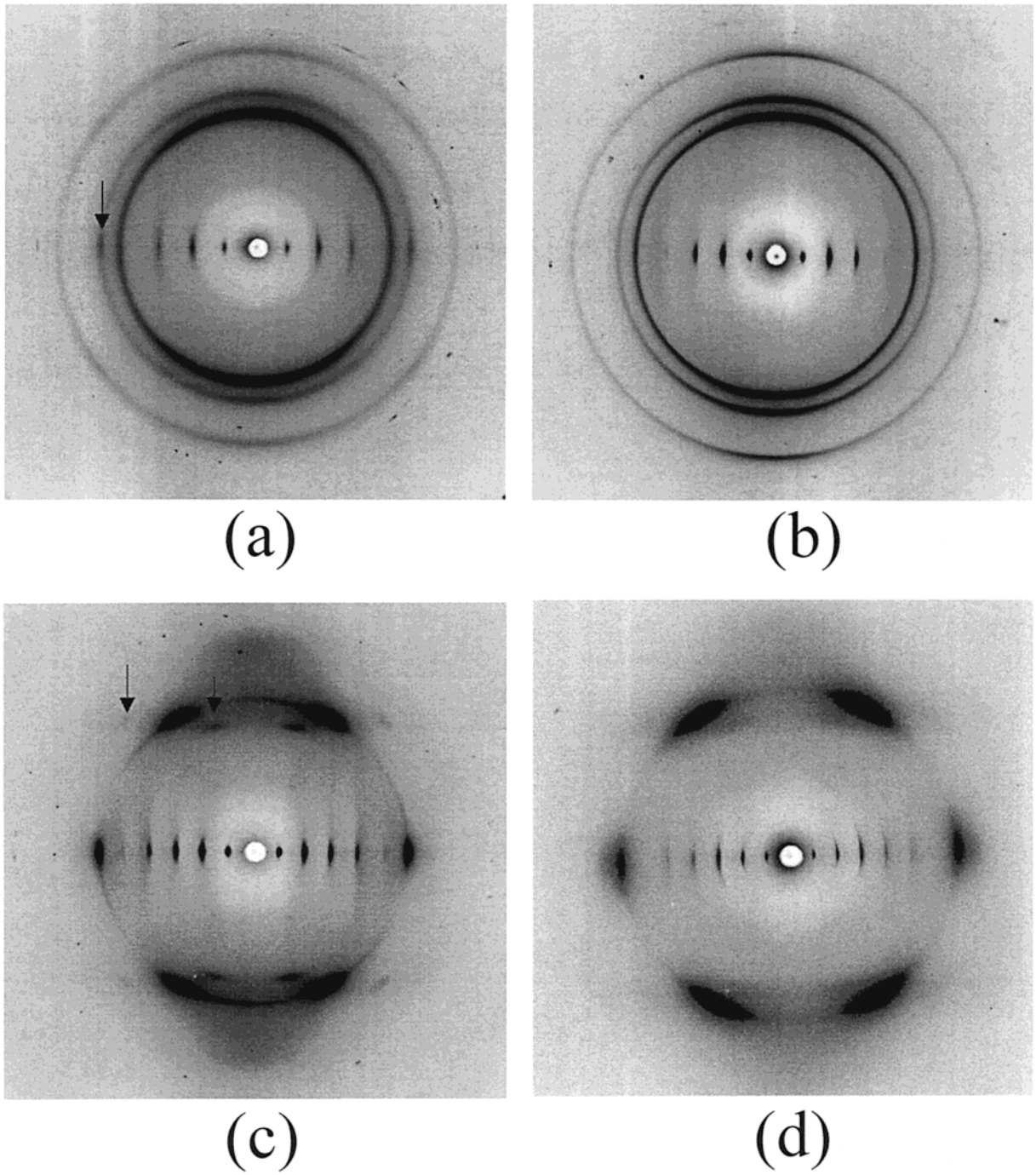

Figure 3. X-ray fiber patterns of as-drawn fibers of (a) PSM-3, (b) PSM-6, (c) PSM-8, and (d) PSM-11.

X-ray Fiber Patterns. Figure 3a shows the X-ray pattern of PSM-3 for a fiber drawn from the isotropic state. There is a series of sharp reflections along the equator and several reflections in the wide-angle region having increased intensity on the meridian. The *d*-spacings are listed in Table 2. The equatorial reflections are orders of the 18.6 Å reflection, indicating a layered smectic structure with thickness of 18.6 Å. In the wide-angle region, six reflections were observed, the first three being stronger than the latter three. (The latter three can hardly be seen in Figure 3a, but they can be seen by controlling contrast in the digital image.) The second of these (marked as an arrow in Figure 3a) has slightly enhanced intensity on both the meridian and equator. It is not an order of the smectic layered spacing. These reflections can be indexed on the basis of a two-dimensional orthorhombic unit cell with dimensions of $a = 8.14$ Å and $b = 5.42$ Å (as shown in Table 2). Strong *110* and *200* reflections are observed while *100* and *010* reflections are not. The absence of the *100* and *010* reflections strongly suggests a two-chain unit cell, with the second possibly positioned in the middle of the cell. However, the appearance of other weak reflections with indices $h + k =$ odd indicates that there is not perfect *C*-centered symmetry. This orthorhombic unit cell is indicative of a S_E structure, the mesogens being packed in an orthorhombic cell within the layers. The basal area of the unit cell is 44.1 Å^2, nearly equivalent to that of other smectic E (S_E) structures (44.4 Å^2) formed by similar mesogens (methoxybiphenyl).[14,15]

Figure 3b shows the X-ray pattern of the as-drawn fiber of PSM-6. The *d*-spacings are listed in Table 2.

Table 2. Measured and Calculated *d*-Spacings of PSM-3 and PSM-6

		d_o (Å)		d_c (Å)	
	hkl	PSM-3	PSM-6	PSM-3	PSM-6
small angle	*001*	18.6	23.2	18.6	23.2
	002	9.35	11.5	9.32	11.6
	003	6.23	7.67	6.32	7.73
wide angle	*110*	4.53	4.51	4.51	
	200	4.01	4.07	4.07	
	210	3.26	3.24	3.25	
	020	2.85	2.87	2.71	
	120	2.63	2.58	2.57	
	310	2.42	2.43	2.43	

Table 3. Measured Layer Thickness (L_m) and Calculated Side Chain Length of Si−O−$(CH_2)_n$−O−Ph−Ph (L_c) and L_m/L_c of PSM-*N*s

sample	measured thickness L_m(Å)	calculated length L_c(Å)	L_m/L_c
PSM-3	18.6	17.5	1.06
PSM-6	22.9	21.3	1.08
PSM-8	25.4	23.8	1.07
PSM-11	29.1	27.5	1.06

Again, there is a series of sharp equatorial reflections and several wide angle reflections with enhanced meridional intensity. The equatorial reflections are orders of a 23.1 Å layered smectic structure. In the wide-angle region, the reflections are nearly the same as those seen in PSM-3 (*d* spacing and relative intensity). Thus, there is again a S_E structure with the same dimensions except for the increased layer thickness due to the longer spacer length.

Figure 3c shows the X-ray pattern (4 h exposure) of the as-drawn fiber of PSM-8, taken immediately after drawing from the isotropic state. The series of ordered sharp reflections on the equator indicates a highly ordered smectic structure with layer thickness of 25.4 Å. Reflections at $d = 5.08$ and 3.68 Å (marked with arrows in Figure 3c) and diffuse scattering along the meridian were also observed and will be discussed later. In the wide-angle region, six diffraction spots are observed at $d = 4.42$ Å and separated by 60° azimuthal angles. The hexagonal six-point pattern indicates a S_B structure with mesogens normal to the drawing direction and packed in a hexagonal array. This hexagonal packing can be expressed alternatively as a two-dimensional orthorhombic unit cell with dimensions $a = 8.8$ Å and $b = 5.08$ Å. Of the six spots, the two on the equator can be indexed as *200*, and the other four can be indexed as *110*. The *200* reflections are weaker than the *110* reflections, indicating preferred orientation in the mesogenic groups. The basal area of the hexagonal cell is 44.7 Å, nearly the same as that of the S_E structures of PSM-3 and PSM-6.

Figure 3d shows the X-ray pattern (4 h exposure) of the as-drawn fiber of PSM-11 obtained immediately after drawing from the isotropic state. Again, there is a series of ordered reflections on the equator and 6-fold reflections at $d = 4.45$ Å. The structure of PSM-11 is very similar to that of PSM-8 but with an increased layer thickness (29.1 Å) due to its increased spacer length.

Smectic Structure. The calculated most extended side chain lengths, L_c, of Si−O−$(CH_2)_n$−O−Ph−Ph are given in Table 3. The L_c values agree well with the measured layer thicknesses, L_m ($L_m/L_c = \sim 1$). Thus, the structures of PSM-*N*s appear to be single-layer arrangements of the mesogens regardless of spacer length. Figure 4 shows the measured layer thickness *vs* the number of methylene units in the spacer. There is a very good linear relationship and a slope of ~1.3 Å per methylene unit. This also indicates a single-layer arrangement; a double-layer structure would be expected to have a slope of ~2.5 Å. Figure 5a,b shows two possible single-layer arrangements viewed parallel to the polymer chain axis. Figure 5a is a true single-layer arrangement, with the pendant groups to one side of the backbone. Figure 5b shows an arrangement with interdigitated pendant groups on both sides of the backbone.[11] Figure 5c shows a side view of the individual

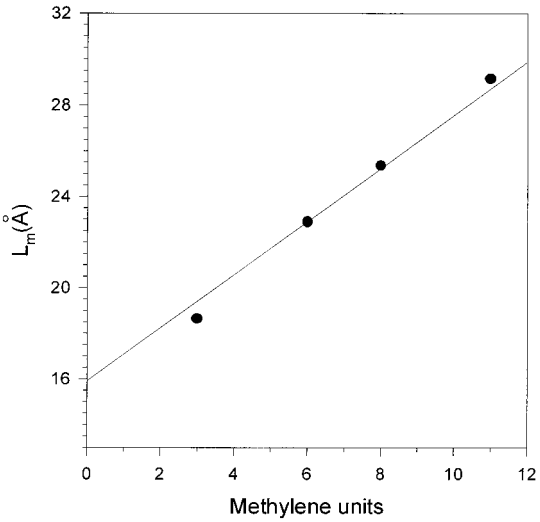

Figure 4. Measured layer thickness *vs* the number of methylene units in the spacer.

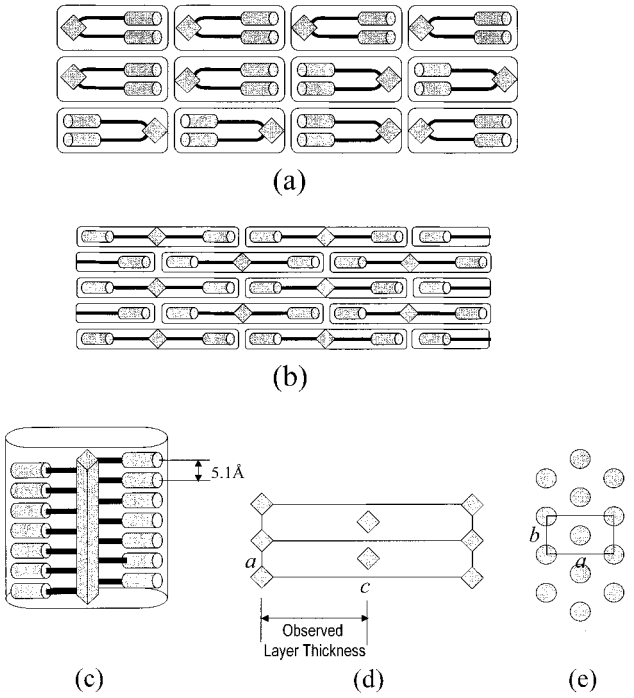

Figure 5. Two possible single-layer arrangements and the projections of the unit cell of PSM-8: (a) true single-layer arrangement, (b) interdigitated arrangement, (c) a side view of an individual layer of (b), (d) the *ac* projection of the unit cell representing (b), and (e) the *ab* projection of the unit cell. (The diamond represents the polymer backbone viewed end-on, the cylinder represents the mesogens, and the heavy black lines represent the spacers.)

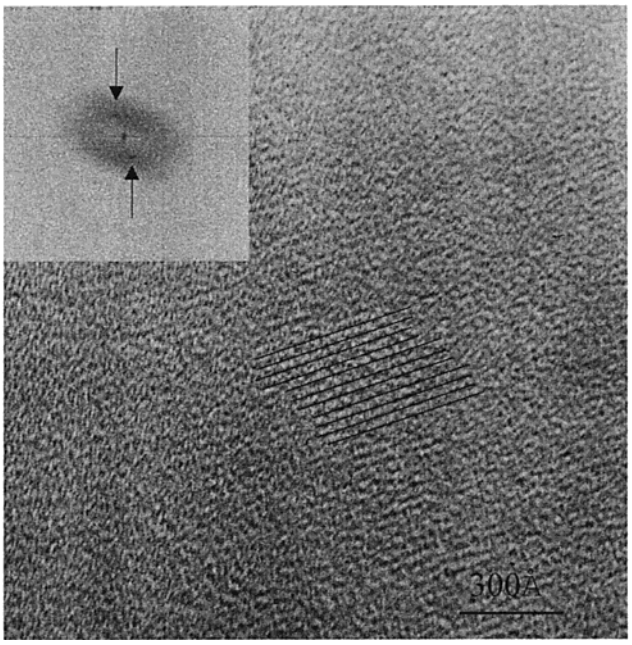

Figure 6. TEM micrograph of PSM-11, stained with RuO_4 and its Fourier transform (inset: white lines represent the layers).

constituent polymer chain comprising the structure shown in Figure 5b.

The main chain conformation for crystalline poly(di-*n*-alkylsilylenemethylene)s is known to be 4_1 helical, accommodating two pendant groups attached to each Si atom.[16] The 4_1 helical structure is energetically favored when the side chains are present because it alleviates steric hindrance. In addition, the fiber repeat of the 4_1 helix, 4.9 Å, is close to the separation distance of side chains along the fiber direction in the PSM-*N*s seen here (5.08 Å, the *b* dimension of the orthorhombic cell for hexagonally packed mesogens, discussed later). In the 4_1 helical structure, the Si atoms are positioned at opposite corners of the square projection of the backbone, and the side chains extend outward from the Si atoms. The model in Figure 5a seems unlikely because it would be very difficult to have all the pendant groups on one side of the backbone for the 4_1 helical structure. Thus, the interdigitated structure appears to be more feasible. Such interdigitation could easily give rise to the 6−8% discrepancies between the layer thicknesses and the side chain lengths seen in Table 3.

Figure 6 shows a TEM image of the smectic layers of PSM-11. The contrast was achieved by staining with RuO_4. The smectic layers in PSM-11 are well-ordered since 5 orders of the layer spacing occur in the X-ray pattern. The layer periodicity can be directly measured in the micrograph and is ∼30 Å comparable to the ∼29 Å small-angle maximum. The extent of the layered structure is large, consistent with the sharp equatorial reflections in the X-ray pattern. The Fourier transformed image (inset in Figure 6) shows the first-order reflection (arrows in Figure 6) and amorphous halo. This sharp first-order reflection clearly indicates that a regular layer structure exists.

Parts a and b of Figure 7 show optical micrographs for PSM-6 and PSM-11, respectively, which were slowly cooled from the isotropic state to room temperature and observed in crossed polaroids. The clear fan-shape focal conic texture for both materials is typical of smectic polymers. This texture was maintained up to the isotropic temperature during heating, indicating that the smectic structure remains during heating. This result agrees with the X-ray data, which show that PSM-11 has a smectic structure up to the isotropic temperature.

Phase Transitions. Figure 8 shows the DSC thermogram of PSM-8 after annealing at room temperature for 1 day. An additional transition at 50 °C has appeared, which was not present in the first cooling and heating cycle. This suggests that very slow crystallization occurs at room temperature. Figure 9a−l shows fiber X-ray patterns at different times and temperatures after drawing. Figure 9a−d shows the fiber X-ray patterns after different lengths of time at room temperature. (Figure 9a is the same as that of Figure 3c, obtained immediately after drawing the fiber and represents the air-quenched structure.) Between 4 and 8 h (during the second exposure) the reflections at 5.08 and 3.68 Å (marked with arrows in Figure 3a) grew stronger, and other new reflections appeared. For example, two new equatorial reflections appeared at $d = 3.90$ and ∼7.8 Å (although the reflection at $d = \sim 7.8$ Å is very diffuse). These also grew stronger during further annealing at room temperature.

Interestingly, many reflections with the same *d* spacing are located at azimuthally different positions. The reflection at $d = 3.68$ Å is originally located ∼45° (azimuthally) from the equator (Figure 9a) but then also appears near the meridian during annealing (Figure 9b). The near-meridian reflection grew stronger with increasing annealing time at room temperature (Figure 9c,d). This reflection became weaker at 35 °C (Figure 9e) and finally disappeared at 45 °C (Figure 9f). The appearance of reflections at different azimuthal positions may be attributed to different orientations in the hexagonal packing of the mesogens. These new reflections could not be indexed as *hk*0 reflections with the two-dimensional orthorhombic cell dimensions of $a = 8.80$ Å and $b = 5.08$ Å (alternative designation for the hexagonal packing). Further, the positions of these reflections in the fiber X-ray pattern are not consistent with hexagonal symmetry. These reflections can only be indexed as *hkl* ($l \neq 0$), indicating the development of three-dimensional order in the layers; i.e., a crystalline structure (K) was formed. (Its detailed indexing will be discussed later.) Above 55 °C, the new wide-angle reflections (*hkl* ($l \neq 0$)) become weaker except for the hexagonal reflections at $d = 4.4$ Å (Figure 9g,h), suggesting that the crystal structure (K) has melted into a S_B phase. The six-point reflections grew more diffuse, and their positions on the meridian at 75 °C indicate that the mesogens have lost their hexagonal order in the layers (Figure 9i,j). However, a layered smectic structure must still remain since the ordered equatorial reflections are little changed in terms of *d*-spacings or relative intensities. The pattern is now typical of a S_A structure. Upon further heating, the structure became isotropic (I) (confirmed by polarized optical microscopy). The S_B structure returned upon cooling from S_A (as shown in Figure 9k by the six-point hexagonal pattern). Further cooling to room temperature again gives crystal structure (K) (Figure 9l). Thus, the phase transitions of PSM-8 during heating occurred as follows:

$$S_{B,\text{quenched}} \xrightarrow{\text{annealing at 25 °C}} K \xrightarrow{55\ °C} S_B \xrightarrow{65\ °C} S_A \xrightarrow{95\ °C} I$$

These temperatures are the DSC measured values.

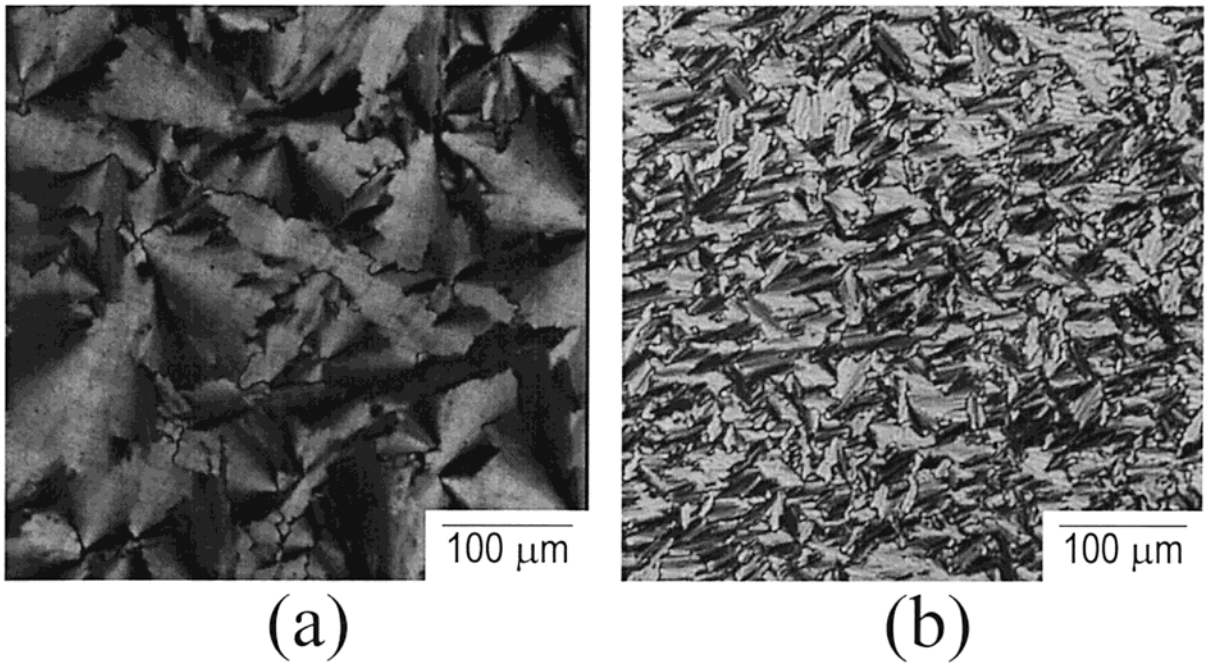

Figure 7. Optical micrographs of (a) PSM-6 and (b) PSM-11 observed under crossed-polarizing filters.

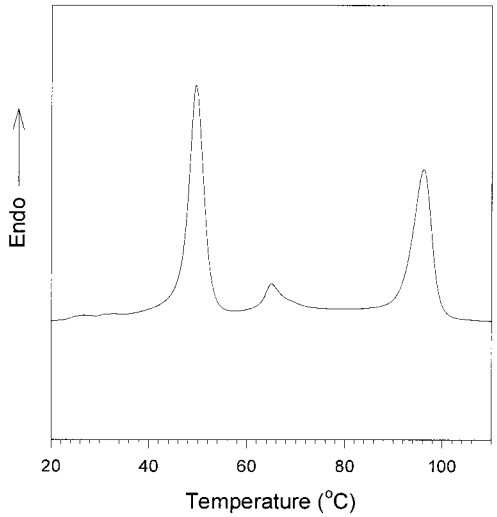

Figure 8. DSC heating thermogram of PSM-8 after initial cooling and heating cycles and subsequent annealing at room temperature for 1 day.

Figure 10a−j shows the X-ray fiber patterns of PSM-11 during annealing at room temperature and while heating. The drawn fiber shows a S_B structure as mentioned earlier for PSM-8 (Figures 10a and 3d). Structural changes similar to those in PSM-8 were observed during annealing at room temperature. A new equatorial reflection observed at $d = 3.93$ Å grew stronger during annealing at room temperature (Figure 10c). Diffraction maxima at $d = 5.10$, 3.77, and 3.18 Å on the first layer line also appeared. Thus, again, a crystalline structure (K) was developed during annealing and heating. These reflections were more intense at 45 °C (Figure 10d), which is near the crystallization temperature seen in DSC. These *hkl* ($l \neq 0$) reflections will be discussed later. Except for the equatorial reflections, there is 6-fold positional symmetry, although the intensities of the six hexagonally arranged reflections are not equal. These wide-angle reflections became weaker at 65 °C (Figure 10g) and at 75 °C blended into a single diffuse scattering maximum positioned on the meridian (Figure 10i). This indicates that the crystal structure transformed to a S_A phase. Upon further heating, the structure became isotropic (I), as confirmed by polarized optical microscopy. The transitions of PSM-11 during heating occurred as follows:

$$S_{B,\text{quenched}} \xrightarrow{42\ ^\circ\text{C}} K \xrightarrow{65\ ^\circ\text{C}} S_A \xrightarrow{92\ ^\circ\text{C}} I$$

The main difference between PSM-8 and PSM-11 is that the crystalline structure of PSM-11 changed directly to S_A whereas the crystalline structure of PSM-8 changed first to S_B and then to S_A.

Crystal Structure. An X-ray fiber pattern was obtained from PSM-8 annealed at 45 °C for 1 day. The *d*-spacings and reciprocal coordinates *R* and *Z* of the observed reflections are listed in Table 4. Equivalent reflections appearing at different azimuthal angles have been omitted. The broad equatorial reflection at $d = \sim 7.8$ Å separated into two reflections at $d = 7.91$ and 7.19 Å during annealing. A meridional reflection was also observed at $d = 2.52$ Å. Since this crystalline structure developed from the S_B phase, it is likely to have hexagonal packing of the side chains. The unit cell dimensions can be calculated from the layer thickness (which gives the *c* dimension) and the hexagonal packing (which gives the *a* and *b* dimensions). (Since the polymer backbone does not contribute significantly to the diffraction pattern, the *c* direction is defined with respect to the liquid crystal side chains rather than along the fiber direction.) PSM-*N*s have a single-layer structure with interdigitated packing in the side chains (as shown in Figure 5b). For this packing model, only *00l* reflections with $l =$ even are possible because of the second chain in the middle of the *ac* plane (Figure 5d). Thus, the actual *c* unit cell dimension must be double the observed layer thickness. The *a* and *b* dimensions from the hexagonal packing are $a = 8.80$ Å and $b = 5.08$ Å in the alternative orthorhombic cell (Figure 5e). The crystal structure of PSM-8 is therefore orthorhombic with unit cell parameters $a = 8.80$ Å, $b = 5.08$ Å, and

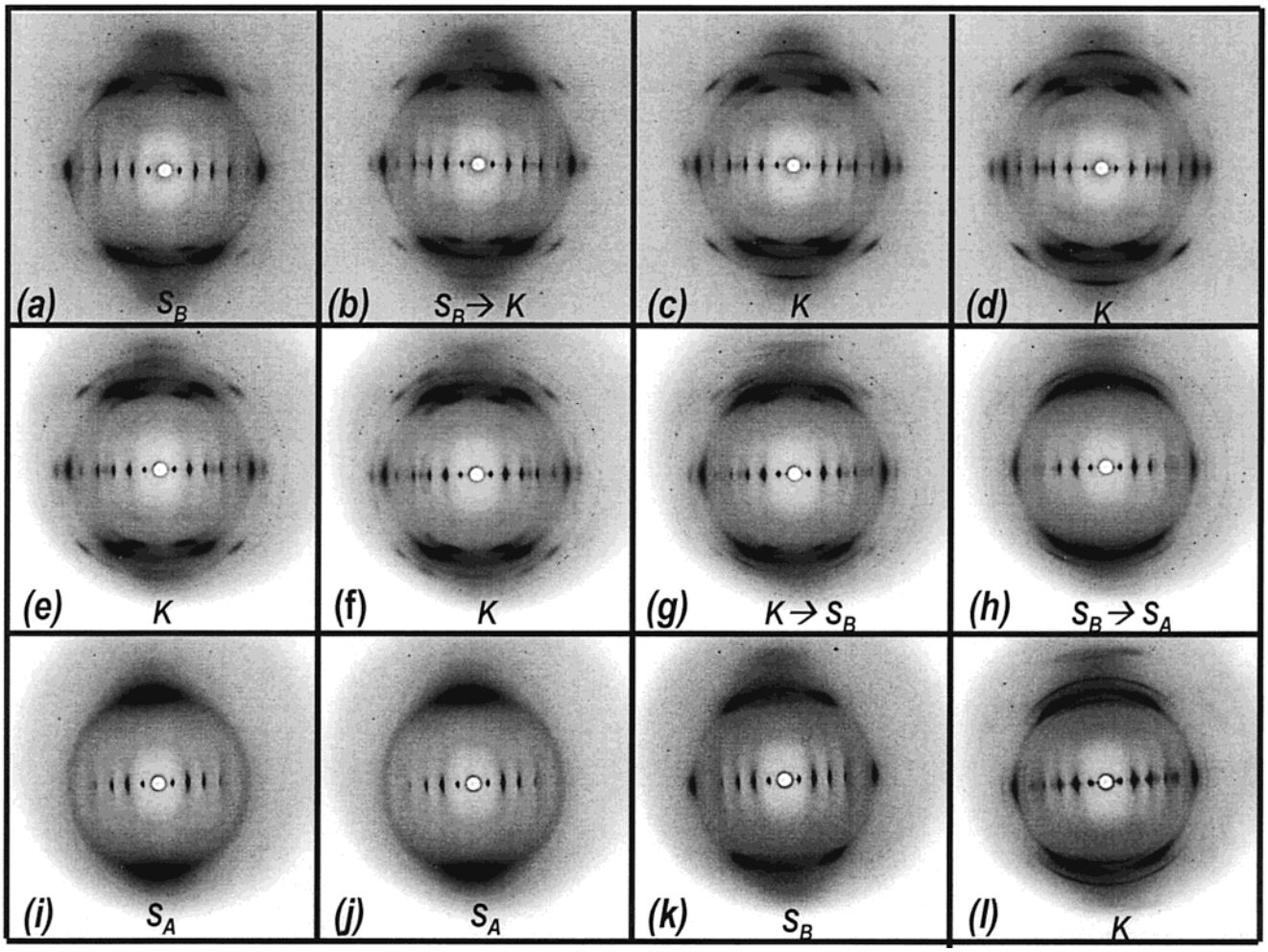

Figure 9. X-ray fiber patterns of PSM-8 at different times and temperatures after drawing: (a) 0−4 h at 25 °C, (b) 4−8 h at 25 °C, (c) 8−23 h at 25 °C, (d) next 23−28 h at 25 °C, (e) 35 °C, (f) 45 °C, (g) 55 °C, (h) 65 °C, (i) 75 °C, (j) 85 °C, (k) cooling to 65 °C, and (l) cooling to 25 °C

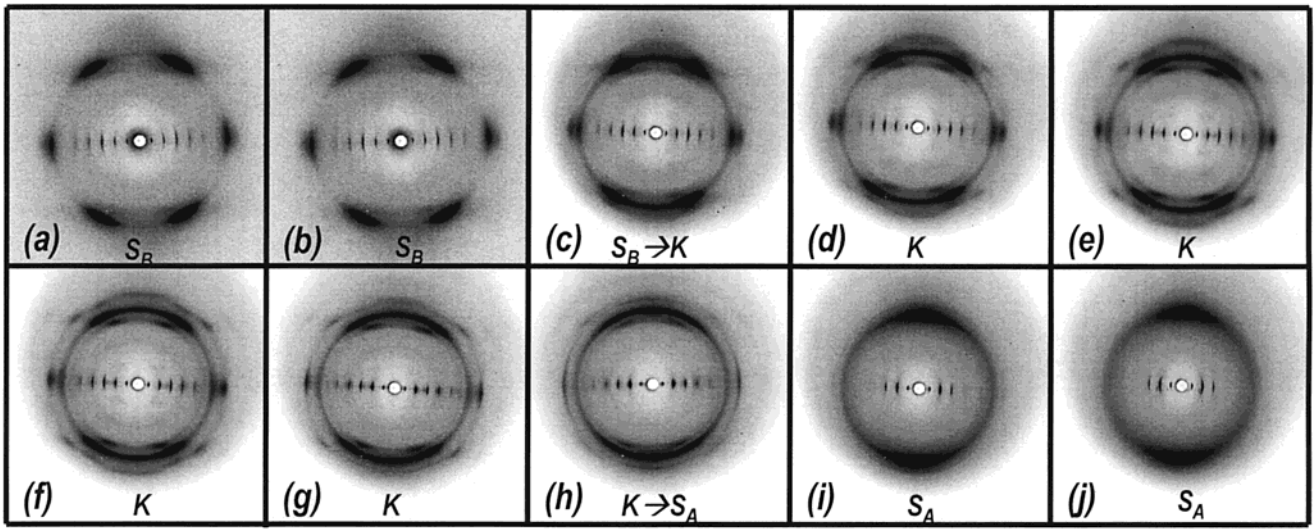

Figure 10. X-ray fiber patterns of PSM-11 at different times and temperatures after drawing: (a) 0−4 h at 25 °C, (b) 4−8 h at 25 °C, (c) after 1 week at 25 °C, (d) 35 °C, (e) 45 °C, (f) 55 °C, (g) 65 °C, (h) 75 °C, (i) 80 °C, and (j) 85 °C.

$c = 50.8$ Å. The equatorial reflections at $d = 7.91$, 7.19, and 3.90 Å are indexed as *103*, *104*, and *206*, respectively. The meridional reflection at $d = 2.52$ Å can be indexed as *020*. Other reflections can be indexed as shown in Table 4. The observed *d*-spacings are in good agreement with calculated values.

The *d*-spacings from the X-ray fiber pattern of PSM-11 annealed at 45 °C are given in Table 5 along with reciprocal *R* and *Z* coordinates. Equivalent reflections appearing at the different azimuthal angles have again been omitted. There is also a diffuse meridional reflection at $d = \sim 2.6$ Å. The unit cell parameters of PSM-11

Table 4. Observed and Calculated *d*-Spacings of PSM-8

h	*k*	*l*	*R* (Å^{-1})	*Z* (Å^{-1})	d_o (Å)	d_c (Å)
0	*0*	*2*	0.039	0	25.4	25.4
0	*0*	*4*	0.078	0	12.8	12.7
0	*0*	*6*	0.118	0	8.47	8.47
1	*0*	*3*	0.126	0	7.91	7.81
1	*0*	*4*	0.139	0	7.19	7.23
0	*0*	*8*	0.157	0	6.36	6.35
0	*0*	*10*	0.196	0	5.09	5.08
2	*0*	*0*	0.227	0	4.40	4.40
2	*0*	*6*	0.256	0	3.90	3.90
0	*1*	*1*	0.069	0.185	5.08	5.05
0	*1*	*3*	0.082	0.190	4.87	4.87
1	*1*	*0*	0.111	0.197	4.42	4.40
1	*1*	*7*	0.194	0.190	3.68	3.76
1	*1*	*8*				3.62
0	*2*	*0*	0	0.397	2.52	2.54

Table 5. Observed and Calculated *d*-Spacings of PSM-11

h	*k*	*l*	*R* (Å^{-1})	*Z* (Å^{-1})	d_o (Å)	d_c (Å)
0	*0*	*2*	0.034	0	29.3	29.3
0	*0*	*4*	0.069	0	14.6	14.7
0	*0*	*6*	0.103	0	9.74	9.77
0	*0*	*8*	0.137	0	7.31	7.33
0	*0*	*10*	0.172	0	5.82	5.86
2	*0*	*0*	0.221	0	4.52	4.45
2	*0*	*7*	0.254	0	3.93	3.93
0	*1*	*1*	0.078	0.180	5.10	5.12
1	*1*	*0*	0.123	0.188	4.45	4.45
1	*1*	*8*	0.195	0.180	3.77	3.80
2	*1*	*6*	0.260	0.177	3.18	3.18
0	*2*	*0*	0	0.378	2.64	2.57

are $a = 8.90$ Å, $b = 5.14$ Å, and $c = 58.6$ Å, calculated in the same way as those of PSM-8. All reflections can be indexed with these unit cell parameters except for three weak reflections at $d = 13.2$, 10.9, and 7.66 Å, which appear on the layer lines at $Z = 0.054$ Å^{-1} ($z = 18.5$ Å) for first two reflections and at $Z = 0.111$ Å^{-1} ($z = 9.00$ Å) for the last one. The layer line spacings of these three reflections ($z = 18.5$ and 9.0 Å) do not have a common value with the layer spacing of other reflections ($z = 5.1$ and 2.6 Å). Thus, the reflections at $d = 13.2$, 10.9, and 7.66 Å may come from another crystalline form.

4. Conclusions

The structures of four side chain liquid crystalline poly(silylenemethylene)s ($-(SiCH_3R-CH_2)-$: R = $O(CH_2)_NO-Ph-Ph$; Ph = phenyl) have been studied by X-ray diffraction, DSC, polarized optical microscopy, and TEM methods. DSC results show that PSM-*N*s have several thermal transitions, dependent on the side chain length. The number of transitions tends to increase as side chain length increases. All PSM-*N*s show a series of sharp equatorial reflections in the X-ray fiber pattern at room temperature, characteristic of well-ordered smectic phases. The layer thickness corresponds to the length of the single side chain and increases with slope of ~1.3 Å per methylene spacer, suggesting a single-layer structure. The mesogens in the side chains of PSM-3 and PSM-6 are packed in a two-dimensional orthorhombic S_E structure with dimensions of $a = 8.14$ Å and $b = 5.14$ Å. The mesogens of PSM-8 and PSM-11 are packed in a hexagonal S_B cell at room temperature. Annealing PSM-8 and PSM-11 at room temperature or slightly above room temperature results in crystallization. The crystal structures are orthorhombic with unit cell parameters for PSM-8 of $a = 8.80$ Å, $b = 5.08$ Å, and $c = 50.8$ Å. Those for PSM-11 are $a = 8.90$ Å, $b = 5.14$ Å, and $c = 58.6$ Å. Upon heating, the crystalline structure of PSM-11 changes to smectic A (S_A) before becoming isotropic. The micrograph of PSM-11 shows a layered structure with thickness matching that observed in the X-ray pattern.

Acknowledgment. Support from the National Science Foundation through Grant DMR-9731345 is gratefully acknowledged. S.-Y. Park also acknowledges support from the Air Force Office of Scientific Research for an NRC postdoctoral research associateship. We thank R. Wheeler at Universal Energy Systems, Inc., for useful discussions about TEM images.

References and Notes

(1) Mcardle, C. B. *Side Chain Liquid Crystal Polymers*; Blackie and Son Ltd.: Glasgow, 1989.
(2) West, R. J. *Chem. Educ. Organosilicon Chem., Parts I and II* **1980**, *57*, 165.
(3) Finkelmann, H.; Rehage, G. *Adv. Polym. Sci.* **1984**, *60/61*, 99.
(4) Rushkin, I.; Interrante, L. V. *Macromolecules* **1996**, *29*, 3123.
(5) Interrante, L. V.; Liu, Q.; Rushkin, I.; Shen, Q. *J. Organomet. Chem.* **1996**, *521*, 1.
(6) Rushkin, I.; Interrante, L. V. *Macromolecules* **1996**, *29*, 5784.
(7) Tsao, M. W.; Rabolt, J.; Farmer, B. L.; Interrante, L. V.; Shin, Q. *Macromolecules* **1996**, *29*, 7130.
(8) Levin, G.; Carmichael, J. B. *J. Polym. Sci.* **1968**, *6*, 1.
(9) Zhang, T.; Park, S. Y.; Farmer, B. L.; Interrante, L. V. *Polym. Prepr.* **2000**, *41* (1), 975; submitted to *Macromolecules*.
(10) Platè, N. A. *Liquid-Crystal Polymers*; Plenum Press: New York, 1993; Chapter 6, p 222.
(11) Gray, G. W.; Goodby, J. W. G. *Smetic Liquid Crystals*; Leonard Hill [Blackie]: Glasgow, 1984.
(12) Cheng, S. Z. D.; Yoon, Y.; Zhang, A.; Savitski, E. P.; Park, J. Y. *Macromol. Rapid Commun.* **1995**, *16*, 533.
(13) Yoon, Y.; Zhang, A.; Ho, R.-H.; Cheng, S. Z. D.; Percec, V.; Chu, P. *Macromoelcules* **1996**, *29*, 294.
(14) Duran, R.; Guillon, D.; Gramain, P.; Skoulios, A. *Makromol. Chem., Rapid Commun.* **1987**, *8*, 181.
(15) Frère, Y.; Yang, F.; Gramain, P.; Guillon, D.; Skoulio, A. *Makromol. Chem.* **1988**, *189*, 419.
(16) Park, S. Y.; Interrante, L. V.; Farmer, B. L. *Polymer* **2001**, *42*, 4253.

MA010449S